Implantable Self-Powered Low-Level Laser Cure System for Mouse Embryonic Osteoblasts' Proliferation and Differentiation

Wei Tang,[†,⊥] Jingjing Tian,[†,⊥] Qiang Zheng,[†] Lin Yan,[‡] Jiangxue Wang,[‡] Zhou Li,[*,†] and Zhong Lin Wang[*,†,§]

[†]Beijing Institute of Nanoenergy and Nanosystems, Chinese Academy of Sciences, Beijing 100083, China, [‡]School of Biological Science and Medical Engineering, Beihang University, Beijing 100191, China, and [§]School of Material Science and Engineering, Georgia Institute of Technology, Atlanta, Georgia 30332-0245, United States. [⊥]W.T. and J.T. contributed equally to this work.

ABSTRACT Bone remodeling or orthodontic treatment is usually a long-term process. It is highly desirable to speed up the process for effective medical treatment. In this work, a self-powered low-level laser cure system for osteogenesis is developed using the power generated by the triboelectric nanogenerator. It is found that the system significantly accelerated the mouse embryonic osteoblasts' proliferation and differentiation, which is essential for bone and tooth healing. The system is further demonstrated to be driven by a living creature's motions, such as human walking or a mouse's breathing, suggesting its practical use as a portable or implantable clinical cure for bone remodeling or orthodontic treatment.

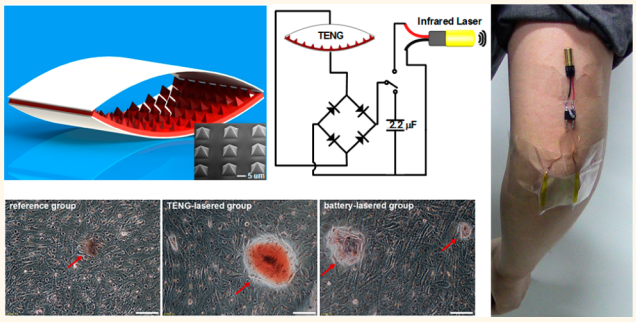

KEYWORDS: self-powered · low-level laser · embryonic osteoblast · proliferation · differentiation

Bone remodeling or orthodontic treatment is usually a long-term process.[1,2] Currently, it is accepted that low-level laser therapy has a positive effect on the speed and quality of this process,[3−5] possibly because the laser's energy corresponds with the characteristic energy and absorption levels of the respiratory chain in mitochondria. Thus, it enhances the vitality actions of cells and accelerates regeneration of the damaged tissues.[2] To facilitate the applications of this technology, an attachable or implantable laser cure system is demanded. However, a normal battery would not work in this scenario because it is either too big in volume or uncomfortable for the patients.

Recently, the invention of the triboelectric nanogenerator (TENG) has provided an effective approach to convert ambient mechanical energy into electricity.[6−14] The working principle of the TENG is based on the combination of contact electrification and electrostatic induction. It has been systematically studied to drive hundreds of light-emitting diodes (LEDs)[15,16] or charging a lithium-ion battery[17] for powering some electronic devices. The TENG has been employed to collect energy from the mouse's breathing to power a pacemaker.[18,19]

In this paper, a self-powered low-level laser cure (SPLC) system for osteogenesis was developed, which significantly accelerated the mouse embryonic osteoblasts' proliferation and differentiation. Moreover, it was found that the system could also work under the drive of a living creature's motions, such as human walking or a mouse's breathing. This work shows great progress not only for TENGs' applications in portable or implantable medical devices but also for clinical therapy of bone remodeling and orthodontic treatment.

RESULTS AND DISCUSSION

The SPLC system is composed of a flexible TENG and an infrared laser excitation unit. The fabrication of the TENG refers to the arch-shaped highly flexible device.[20] Polydimethylsiloxane (PDMS) and indium tin

* Address correspondence to zli@binn.cas.cn, zlwang@binn.cas.cn.

Received for review June 12, 2015 and accepted July 10, 2015.

Published online July 10, 2015
10.1021/acsnano.5b03567

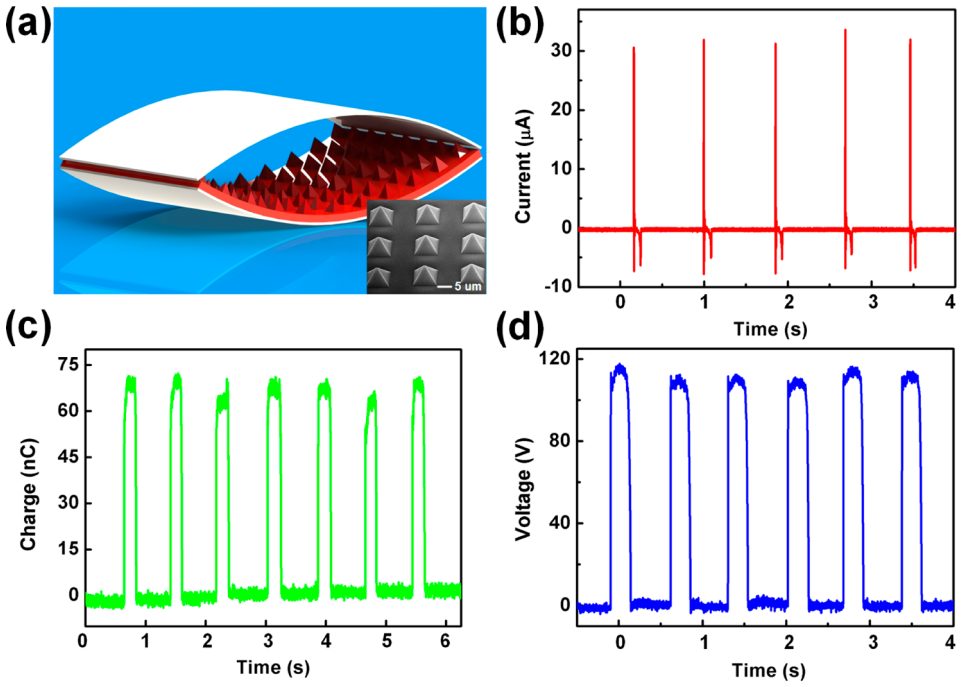

Figure 1. Structural design and characterizations of the TENG. (a) Schematic illustrations of the flexible arch-shaped TENG. (b) Short-circuit current, (c) transferred charge, and (d) open-circuit voltage of the as-fabricated TENG.

oxide (ITO) were utilized as the friction materials. However, to enhance the TENG's current output, a pyramid array patterned PDMS film was preferred[16] instead of the plain film (Figure 1 a). It consists of a pyramid array with each side's length being 5 μm. The working principle of this TENG was previously reported and is based on the combination of contact electrification and electrostatic induction. The electric characterizations were measured by a Keithley 6514 system electrometer and a SR570 low-noise current amplifier from Stanford Research Systems. Testing results are shown in Figure 1b−d. The TENG output a short-circuit current of about 30 μA and an open-circuit voltage of 115 V. The transferred charge during one period was around 70 nC.

As for the biological experiment, murine calvarial preosteoblasts (MC3T3-E1) (ATCC CRL-2594) were chosen. It is a mouse calvaria-derived cell line that can provide a useful *in vitro* system to study the different stages during the osteoblast differentiation.[21] The cells were initially cultured with DMEM (Dulbecco's modified Eagle's medium, with 10% fetal bovine serum and 1% penicillin−streptomycin) in 5% CO_2 at 37 °C, seeded in 96-well plates for 3000 cells/100 μL, and allocated in three groups: reference group—no laser treatment; laser-irradiated group driven by TENG (TENG-lasered group)—pulse laser irradiation driven by TENG (100 pulses/day); laser-irradiated group using a battery (battery-lasered group)—continuous laser irradiation powered by a battery (1 min/day), as shown in Figure 2a. Before laser treatment, all of the cells were incubated for 24 h. Then, the laser treatment was performed, and cells were tested after another 24 h of incubation. During the incubating process, we covered the whole plates with tinfoil to avoid any ambient illumination.

For the infrared laser, it has a wavelength and power of 850 nm and 10 mW, with an irradiation diameter of 6 mm, which means the power density is about 35.4 mW/cm^2. The TENG-lasered irradiation was driven by the TENG with a capacitor as an electricity reservoir (Figure 2b). The TENG was triggered by a motor with a displacement of ±0.5 mm and a frequency of 50 Hz. The infrared signals for the two laser groups are shown in Figure 2c,d.

Since MC3T3-E1 becomes functional during the successive developmental stages, including the proliferation period, bone matrix formation, and mineralization stages,[21,22] in the following experiments, we used a MTT [3-(4,5-dimethylthiazol-2-yl)-2,5-diphenyltetrazolium bromide] test to assess cell proliferation, ALP (alkaline phosphatase) level to detect early bone matrix formation, and Alizarin red S dye to characterize the mineralization.

To investigate the effect of infrared irradiation on MC3T3-E1, we stained the cytoskeleton and nucleus with phalloidin and DAPI (Sigma-Aldrich) to observe the morphology and quantity of cells, as shown in Figure 3. Phalloidin (red) specifically binds to cellular filamentous actin, which displayed the relative integrity of the cytoskeleton. There was no distortion of the cytoskeleton structure observed among the three groups, which implied that the cells in TENG-lasered (Figure 3b,e,h, 1−3 days) and battery-lasered

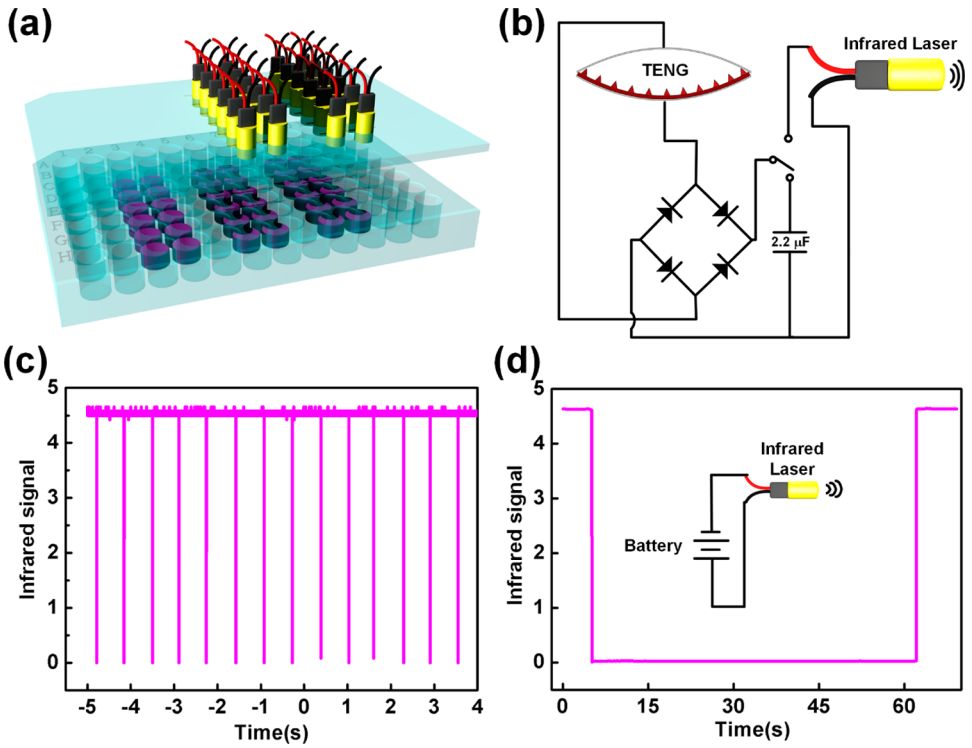

Figure 2. (a) Bioexperimental setup. (b) Schematic diagram of the SPLC system. (c) Infrared laser signal emitted by the SPLC system. (d) Infrared laser signal emitted by a battery.

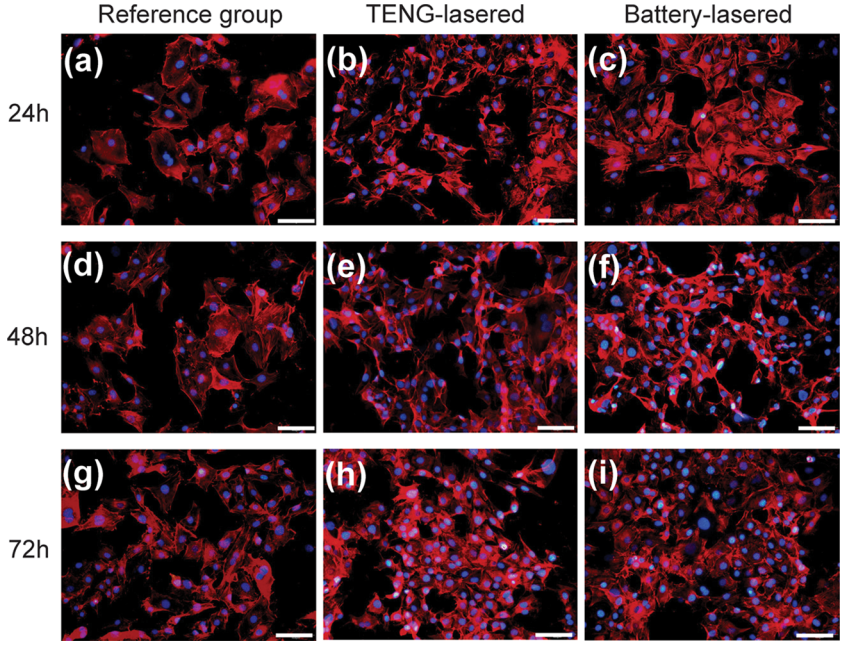

Figure 3. Quantity and morphology of the MC3T3-E1 cell with different processing methods, stained by phalloidin and DAPI. (a,d,g) Reference group cultured 24, 48, and 72 h, respectively. (b,e,h) TENG-lasered group, with the irradiation dose of 100 pulses/day, cultured 24, 48, and 72 h, respectively. (c,f,i) Battery-lasered group, with the irradiation dose of 1 min/day, cultured 24, 48, and 72 h, respectively. Scale bar is 100 μm.

irradiation groups (Figure 3c,f,i, 1−3 days) grew as normal as the reference group. Additionally, DAPI (blue) specifically binds to the DNA of the nucleus. The quantity of nucleus in all irradiated groups increased compared to that in the reference group (Figure 3a,d,g, 1−3 days), which means the cells proliferated apparently under infrared irradiation.

After being plated, the cells entered a proliferative phase.[23] Proliferation was evaluated at 24 h after laser irradiation and assessed using the MTT assay. After

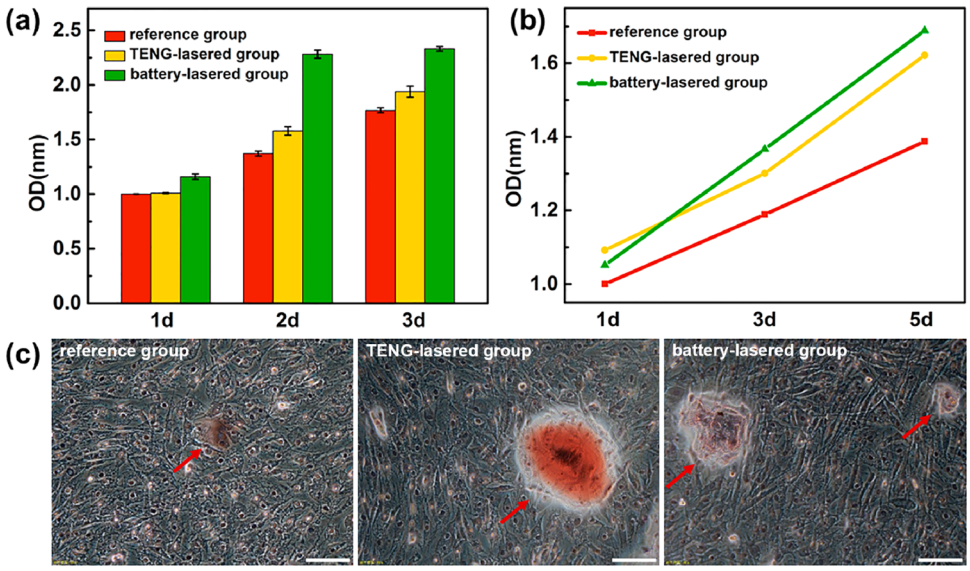

Figure 4. (a) MTT results show a promotion on the proliferation of MC3T3-E1 after different laser irradiation. The cell viability of the TENG-lasered group was 15 and 10% higher than that of the reference group, respectively, after being irradiated for 2 and 3 days. Battery-lasered group was 66 and 32% higher. (b) ALP level and (c) mineral deposition results implied that the laser irradiation could induce bone formation. The ALP level of the TENG-lasered group for 1, 3, and 5 day treatment was 9.2, 9.4, and 16.9% higher than that of reference group, respectively. Battery-lasered group was 5.1, 15.0, and 21.7% higher. The mineralized area in both TENG-lasered and battery-lasered groups was significantly larger than that in the reference group. The mineralized area is marked with a red arrow, which was stained by Alizarin red S. Scale bar is 100 μm.

10 μL of MTT (0.5 mg/mL in final concentration) was added per well, cells were incubated in the dark for another 4 h in 5% CO_2 at 37 °C to induce the production of formazan crystals. One hundred microliters of dimethylsulfoxide was added to dissolve the aforementioned formazan crystals. Absorbance was read at 490 nm to evaluate the cell proliferation on an enzyme-linked immunosorbent assay (ELISA) reader. As shown in Figure 4a, after treatment with infrared irradiation for 1 day, there was no significant difference observed in the reference, TENG-lasered, or battery-lasered irradiation groups. However, after irradiation by an infrared laser for 2 or 3 days, the cells in the irradiated groups increased statistically remarkably. Specifically, the cell viability of the TENG-lasered group was 15 and 10% higher than that of the reference group for the 2 day and 3 day samples, respectively. The cell viability of the battery-lasered group was 66 and 32% higher than that of the reference group, respectively. Our results indicated that the TENG-lasered and battery-lasered irradiation could promote cell proliferation.[24]

The ALP level indicates the beginning of bone matrix synthesis and the maturity of the extracellular matrix of the MC3T3-E1 cell.[23,25−27] The extracellular ALP level was measured with an ALP ELISA kit. This kit adopted a double sandwich method. The absorbance was read at 450 nm (Figure 4b) on an ELISA reader. The cell culture time was relatively longer than the proliferation test, and the irradiation times also increased. We measured the ALP level (Figure 4b) of three groups after 1, 3, and 5 days of irradiation. The TENG-lasered group was 9.2, 9.4, and 16.9% higher than the reference group, respectively, and the battery-lasered group was 5.1, 15.0, and 21.7% higher than the reference group. The ALP level implied that the bone matrix synthesis was activated by the infrared irradiation and the MC3T3-E1 cells had a more mature extracellular matrix after laser treatment.

Mineral deposition is a significant marker of bone formation *in vivo* in MC3T3-E1 cells,[21] which will begin after several days of induction. Here, we added 50 μg/mL ascorbic acid (AA) and 10 mM β-glycerophosphate into DMEM to induce mineral deposition of MC3T3-E1 cells. We used the Alizarin red S method to evaluate the mineral deposition of MC3T3-E1 cells at day 28 (Figure 4c). After being stained by Alizarin red S, the optical images showed obvious mineral deposition in the infrared irradiation groups. Both the quantity of calcium nodules and mineralized area in both TENG-lasered and battery-lasered irradiation groups were obviously larger than those in the reference group (Figure 4c and Supporting Information Table S1).[28,29]

In all, our experiments significantly demonstrated that the TENG-lasered treatment had a positive effect on osteoblasts' proliferation, differentiation, and bone formation. Compared to the continuous irradiation powered by a battery, the pulse irradiation powered by the SPLC system has a similar effect, consistent with previous work.[30−32] Additionally, it is more convenient for portable or implantable clinical treatment.

Subsequently, the dose of infrared irradiation was further optimized in our experiment (Figure 5). The TENG-lasered group was irradiated by a TENG-powered infrared

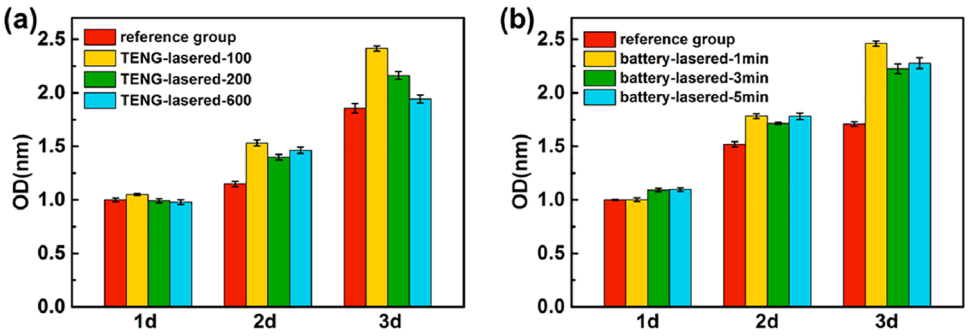

Figure 5. MTT results revealed cell proliferation of MC3T3-E1 with various doses of TENG-lasered (a) and battery-lasered (b) irradiation. The reference group was without irradiation. The TENG-lasered-100, -200, and -600 were irradiated for 100, 200, and 600 pulses per 24 h by a TENG-powered laser, respectively. The battery-lasered-1, -3, and -5 min were irradiated for 1, 3, and 5 min per 24 h by a DC-powered laser, respectively.

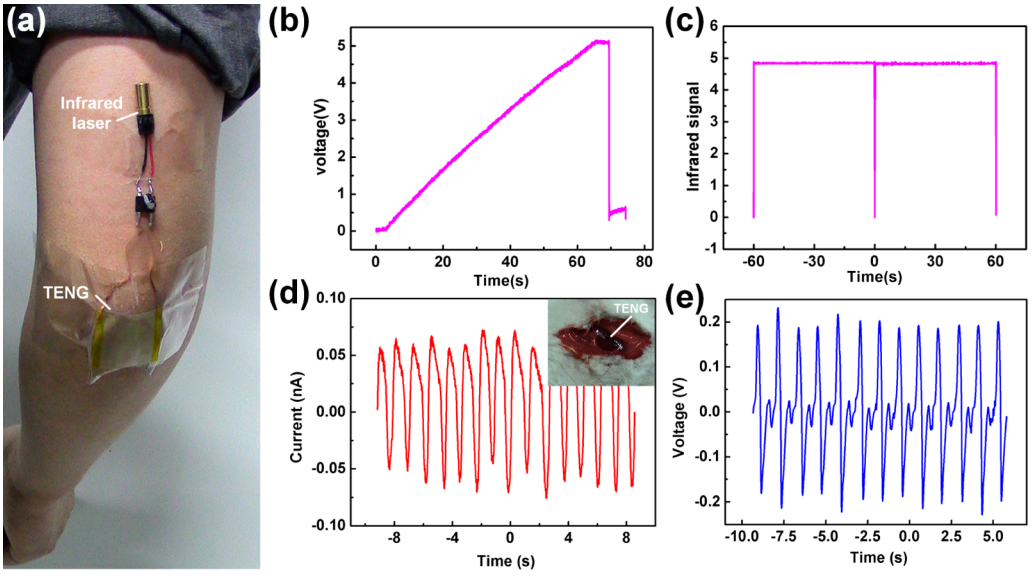

Figure 6. SPLC system was demonstrated to work in living creatures. (a) SPLC system was attached to an arm. (b) Voltage curve of the capacitor in the circuit. (c) Infrared signals of the system. (d,e) Typical current and voltage output of the TENG that was implanted between the diaphragm and liver of a rat.

laser for 100, 200, and 600 pulses per day. The battery-lasered group was irradiated by a DC-powered infrared laser for 1, 3, and 5 min per day. The cell proliferation was detected, and testing results showed that cells grew better in the 100 pulses/day and 1 min/day infrared irradiation group. The dose of 100 pulses or 1 min infrared irradiation per day might be an efficient method for cure application.

To demonstrate the practical potential of the self-powered low-level laser cure system, we fixed it in living creatures. As shown in Figure 6a, it was attached to the arm. As the arm swung during walking, the TENG was triggered and charged the 2.2 μF capacitor to 5 V within 60 s (Figure 6b). Afterward, the laser was excited (Figure 6c). That means the attached SPLC system can work well, driven by a human's normal walking, with a laser irradiation rate of 1 pulse/min (Supporting Information video S1).

Additionally, we investigated the possibility of implanting the SPLC system. The size of the TENG in the implanted experiment (iTENG) was strictly limited to 1.5 cm $\times$ 1.0 cm because the animal is small, which would limit the iTENG's output. Adult rats (Hsd: Sprague-Dawley SD, 150−200 g) were used in this experiment. The anesthesia procedure included the intake of isoflurane gas (1−3% in pure medical grade oxygen) for anesthesia induction and injection of 1% sodium pentobarbital (intraperitoneal, 40 mg/kg) for anesthesia maintenance. A tracheotomy was then performed, and a tracheal intubation was connected to a respirator, which provided artificial respiration and sustained the life of the rat. Then, an iTENG (1.5 cm $\times$ 1.0 cm) was implanted between the diaphragm and the liver, as shown in Figure 6d. The inhalation and exhalation of the rat conducts a regular motion of the diaphragm, which extruded the iTENG periodically. The deformation of the iTENG caused the contacting and separation between the ITO layer and the PDMS film, which generated electric energy. The typical short-circuit current and open-circuit voltage

of the iTENG were 0.06 nA and 0.2 V, respectively (Figure 6d,e). The current and voltage were detected *in vivo*, and the breath of the rat was driven by the respirator at a constant rate of about 50 times/min (Supporting Information video S2).

CONCLUSIONS

In summary, we developed a self-powered low-level laser cure system for osteogenesis, based on the integration of a triboelectric nanogenerator and an infrared laser irradiation unit. It was demonstrated that the system enhanced MC3T3-E1 proliferation by 15% after 2 days of laser irradiation and accelerated the cells' differentiation by 16.9% after 5 days of irradiation. Osteoblast mineralization was also significantly increased by the SPLC system. In addition, we applied it on the human body and found that the infrared laser was successfully excited after 1 min of walking. This work shows a great progress not only for application of TENGs in portable or implantable medical devices but also for clinical therapy of bone remodeling and orthodontic treatment.

Conflict of Interest: The authors declare no competing financial interest.

Acknowledgment. We thank the "Thousands Talents" program for pioneer researcher and his innovation team, China (NSFC 31200702), the Beijing Natural Science Foundation of China (4141002, 7132121) and the China Postdoctoral Science Foundation (2014M550031), Beijing Nova Program (Z121103002512019), and Beijing Municipal Science & Technology Commission (Z131100006013004) for the support.

Supporting Information Available: Image, average quantity, and area of mineral deposition results. The Supporting Information is available free of charge on the ACS Publications website at DOI: 10.1021/acsnano.5b03567.

REFERENCES AND NOTES

1. Pretel, H.; Lizarelli, R. F.; Ramalho, L. T. Effect of Low-Level Laser Therapy on Bone Repair: Histological Study in Rats. *Lasers Surg. Med.* **2007**, *39*, 788–796.
2. Jawad, M. M.; Husein, A.; Alam, M. K.; Hassan, R.; Shaari, R. Overview of Non-Invasive Factors (Low Level Laser and Low Intensity Pulsed Ultrasound) Accelerating Tooth Movement During Orthodontic Treatment. *Lasers Med. Sci.* **2014**, *29*, 367–372.
3. Luger, E. J.; Rochkind, S.; Wollman, Y.; Kogan, G.; Dekel, S. Effect of Low-Power Laser Irradiation on the Mechanical Properties of Bone Fracture Healing in Rats. *Lasers Surg. Med.* **1998**, *22*, 97–102.
4. Khadra, M.; Rønold, H. J.; Lyngstadaas, S. P.; Ellingsen, J. E.; Haanæs, H. R. Low-Level Laser Therapy Stimulates Bone-Implant Interaction: an Experimental Study in Rabbits. *Clin. Oral Impl. Res.* **2004**, *15*, 325–332.
5. Lirani-Galvão, A. P.; Jorgetti, V.; Da Silva, O. L. Comparative Study of How Low-Level Laser Therapy and Low-Intensity Pulsed Ultrasound Affect Bone Repair in Rats. *Photomed. Laser Surg.* **2006**, *24*, 735–740.
6. Wang, Z. L. Triboelectric Nanogenerators As New Energy Technology for Self-Powered Systems and As Active Mechanical and Chemical Sensors. *ACS Nano* **2013**, *7*, 9533–9557.
7. Fan, F. R.; Tian, Z. Q.; Wang, Z. L. Flexible Triboelectric Generator. *Nano Energy* **2012**, *1*, 328–334.
8. Zhang, C.; Tang, W.; Han, C. B.; Fan, F. R.; Wang, Z. L. Theoretical Comparison, Equivalent Transformation, and Conjunction Operations of Electromagnetic Induction Generator and Triboelectric Nanogenerator for Harvesting Mechanical Energy. *Adv. Mater.* **2014**, *26*, 3580–3591.
9. Tang, W.; Han, Y.; Han, C. B.; Gao, C. Z.; Cao, X.; Wang, Z. L. Self-Powered Water Splitting Using Flowing Kinetic Energy. *Adv. Mater.* **2015**, *27*, 272–276.
10. Zhu, G.; Chen, J.; Zhang, T. J.; Jing, Q. S.; Wang, Z. L. Radial-Arrayed Rotary Electrification for High Performance Triboelectric Generator. *Nat. Commun.* **2014**, *5*, 3426.
11. Zhang, X. S.; Han, M. M.; Wang, R. X.; Zhu, F. Y.; Li, Z. H.; Wang, W.; Zhang, H. X. Frequency-Multiplication High-Output Triboelectric Nanogenerator for Sustainably Powering Biomedical Microsystems. *Nano Lett.* **2013**, *13*, 1168–1172.
12. Meng, B.; Tang, W.; Too, Z.; Zhang, X.; Han, M.; Zhang, H. X. A Transparent Single-Friction-Surface Triboelectric Generator and Self-Powered Touch Sensor. *Energy Environ. Sci.* **2013**, *6*, 3235–3240.
13. Yang, Y.; Zhou, Y.; Zhang, H.; Liu, Y.; Lee, S.; Wang, Z. L. A Single-Electrode Based Triboelectric Nanogenerator As Self-Powered Tracking System. *Adv. Mater.* **2013**, *25*, 6594–6601.
14. Tang, W.; Zhang, C.; Han, C. B.; Wang, Z. L. Enhancing Output Power of Cylindrical Triboelectric Nanogenerators by Segmentation Design and Multilayer Integration. *Adv. Funct. Mater.* **2014**, *24*, 6684–6690.
15. Zhu, G.; Lin, Z. H.; Jing, Q. S.; Bai, P.; Pan, C. F.; Yang, Y.; Zhou, Y. S.; Wang, Z. L. Toward Large-Scale Energy Harvesting by a Nanoparticle-Enhanced Triboelectric Nanogenerator. *Nano Lett.* **2013**, *13*, 847–853.
16. Tang, W.; Meng, B.; Zhang, H. X. Investigation of Power Generation Based on Stacked Triboelectric Nanogenerator. *Nano Energy* **2013**, *2*, 1164–1171.
17. Wang, S.; Lin, L.; Wang, Z. L. Nanoscale Triboelectric-Effect-Enabled Energy Conversion for Sustainably Powering Portable Electronics. *Nano Lett.* **2012**, *12*, 6339–6346.
18. Li, Z.; Zhu, G.; Yang, R.; Wang, A. C.; Wang, Z. L. Muscle-Driven *In Vivo* Nanogenerator. *Adv. Mater.* **2010**, *22*, 2534–2537.
19. Zheng, Q.; Shi, B. J.; Fan, F. R.; Wang, X. X.; Yan, L.; Yuan, W. W.; Wang, S. H.; Liu, H.; Li, Z.; Wang, Z. L. *In Vivo* Powering of Pacemaker by Breathing-Driven Implanted Triboelectric Nanogenerator. *Adv. Mater.* **2014**, *26*, 5851–5856.
20. Fan, F. R.; Luo, J.; Tang, W.; Li, C.; Zhang, C.; Tian, Z. Q.; Wang, Z. L. Highly Transparent and Flexible Triboelectric Nanogenerators: Performance Improvements and Fundamental Mechanisms. *J. Mater. Chem. A* **2014**, *2*, 13219–13225.
21. Choi, J. Y.; lee, B. H.; Song, K. B.; Park, R. W.; Kim, I. S.; Sohn, K. Y.; Jo, J. S.; Ryoo, H. M. Expression Patterns of Bone-Related Proteins During Osteoblastic Differentiation in MC3T3-E1 Cells. *J. Cell. Biochem.* **1996**, *61*, 609–618.
22. Sessions, N. D.; Halloran, B. P.; Bikle, D. D.; Wronski, T. J.; Cone, C. M.; Morey-Holton, E. Bone Response to Normal Weight Bearing After a Period of Skeletal Unloading. *Am. J. Physiol-Endoc. Metab.* **1989**, *257*, E606–E610.
23. Wang, D.; Christensen, K.; Chawla, K.; Xiao, G. Z.; Krebsbach, P. H.; Franceschi, R. T. Isolation and Characterization of MC3T3-E1 Preosteoblast Subclones with Distinct *In Vitro* and *In Vivo* Differentiation/Mineralization Potential. *J. Bone Miner. Res.* **1999**, *14*, 893–903.
24. Nogueira, G. T.; Mesquita-Ferrari, R. A.; Souza, N. H. C.; Artilheiro, P. P.; Albertini, R.; Bussadori, S. K.; Fernandes, K. P. S. Effect of Low-Level Laser Therapy on Proliferation, Differentiation, and Adhesion of Steroid-Treated Osteoblasts. *Lasers Med. Sci.* **2012**, *27*, 1189–1193.
25. Franceschi, R. T.; Iyer, B. S.; Cui, Y. Effects of Ascorbic Acid on Collagen Matrix Formation and Osteoblast Differentiation in Murine MC3T3-E1 Cells. *J. Bone Miner. Res.* **1994**, *9*, 843–854.
26. Stein, G. S.; Lian, J. B.; Owen, T. A. Relationship of Cell Growth to the Regulation of Tissue-Specific Gene Expression During Osteoblast Differentiation. *FASEB J.* **1990**, *4*, 3111–3123.
27. Franceschi, R. T.; Iyer, B. S. Relationship Between Collagen Synthesis and Expression of the Osteoblast Phenotype in MC3T3-E1 Cells. *J. Bone Miner. Res.* **1992**, *7*, 235–246.

28. Kim, I. S.; Cho, T. H.; Kim, K.; Weber, F. E.; Hwang, S. J. High Power-Pulsed Nd: YAG Laser As a New Stimulus to Induce BMP-2 Expression in MC3T3-E1 Osteoblasts. *Lasers Surg. Med.* **2010**, *42*, 510–518.
29. Da Silva, A.; Petri, A.; Crippa, G.; Sasso Stuani, A.; Rosa, A. L.; Sasso Stuani, M. B. Effect of Low-Level Laser Therapy After Rapid Maxillary Expansion on Proliferation and Differentiation of Osteoblastic Cells. *Lasers Med. Sci.* **2012**, *27*, 777–783.
30. Stein, A.; Benayahu, D.; Maltz, L.; Oron, U. Low-Level Laser Irradiation Promotes Proliferation and Differentiation of Human Osteoblasts. *Photomed. Laser Surg.* **2005**, *23*, 161–166.
31. Ueda, Y.; Shimizu, N. Effects of Pulse Frequency of Low-Level Laser Therapy (LLLT) on Bone Nodule Formation in Rat Calvarial Cells. *J. Hematother.* **2003**, *21*, 271–277.
32. Khadra, M.; Lyngstadaas, S. P.; Haanæs, H. R.; Mustafa, K. Effect of Laser Therapy on Attachment, Proliferation and Differentiation of Human Osteoblast-Like Cells Cultured on Titanium Implant Material. *Biomaterials* **2005**, *26*, 3503–3509.